Experimental study of liquid line temperature drop as a fault feature for detecting severe liquid line restrictions in residential air conditioning systems

Yifeng Hu, Yuxuan Chen, David P. Yuill

Citation:

Hu, Y., Chen, Y., Yuill, D.P. 2023. Experimental study of liquid line temperature drop as a fault feature for detecting severe liquid line restrictions in residential air conditioning systems, *International Journal of Refrigeration*, 152 (2023), p. 293-302, https://doi.org/10.1016/j.ijrefrig.2023.04.029

Abstract

Liquid line restrictions (LL) can occur in an air conditioning system in multiple ways, such as a clogged filter drier, kinked liquid line, etc., and impact the performance of the system. In this study, the objective is to test and refine fault diagnostic methods for LL faults. We tested the effects of four common installation faults in a laboratory- LL, improper evaporator airflow, improper refrigerant charge, and the presence of non-condensable gas in the refrigerant, singly and in combination. They were tested on a split residential heat pump and an air conditioner in cooling mode. The results are used to validate a method that uses the liquid line temperature drop caused by LL faults as a feature to detect LL faults. The sensitivity of this temperature drop to LL faults and other faults were also studied, so that an effective threshold for declaring an LL fault can be ascertained. The experiments are the first to show that this feature is effective in detecting LL faults even when multiple other faults are present, and that it does not cause false positives when no LL is present.

Keywords: liquid line restrictions, residential air conditioning system, fault detection and diagnosis method, decoupling feature

Nomenclature

Symbols	
Δ	difference
$\dot{m}$	mass flow rate, kg/min
m	mass, kg
P	pressure, kPa
T	temperature, °C
Subscripts	
A	"A" rated condition
actual	actual condition
atm	atmospheric
comp	compressor
EA	evaporator airflow
i	inlet
LL	liquid line restrictions
NOF	fault-free condition
N_2	Nitrogen gas
o	outlet

rated	rated condition
ref	refrigerant
SC	subcooling
Abbreviations	
ASHP	air source heat pump
CH	refrigerant charge (including undercharge and overcharge)
COP	coefficient of performance
EA	improper evaporator airflow
EEV	electronic expansion device
FDD	fault detection and diagnosis
FI	fault intensity
FXO	fixed orifice expansion device
LL	liquid line restrictions
NC	non-condensable gas
OC	refrigerant overcharge
RTU	rooftop unit
SEER	seasonal energy efficiency ratio
TXV	thermostatic expansion valve
UC	refrigerant undercharge

1 Introduction

According to the residential electricity consumption survey (EIA, 2015), the three largest residential electricity consumption categories are air conditioning, space heating, and water heating, accounting for 17%, 15%, and 14% of the total electricity usage in residential sector, respectively, in the United States. Residential air conditioning is primarily provided by air source heat pumps (ASHPs) or unitary cooling air conditioners. Faults can occur during installation of heat pumps and air-conditioners, such as refrigerant overcharge (OC) or the presence of non-condensable gas (NC) in the refrigerant; they can also occur during operating period, like refrigerant leakage; some can occur in both stages, like improper evaporator airflow (EA) or liquid line restrictions (LL).

There are several conditions that are classified as liquid line restrictions. One is a clogged filter-drier. The clog could be impurities or debris (such as brazing material) from before or during installation. Large debris could also clog the inlet to the expansion device. Another is a physical pinch in the liquid line, which can be caused by a kink from a bent line (during or after installation) or other physical constriction. These restrictions cause an unintentional reduction in pressure of the flowing refrigerant. If the restriction is quite severe, it can cause the pressure to drop low enough that phase change occurs.

In air-conditioners equipped with a fixed orifice expansion device (FXO), the restriction causes an unnecessarily high drop in pressure from the high side to low side, reducing the evaporating temperature, which typically causes a lower sensible heat ratio on the air-side of the evaporator and increases compressor work, resulting in loss of efficiency and capacity, as well as unnecessary humidity removal. The restriction can also result in the compressor running at a higher temperature, reducing its working life.

For air-conditioners equipped with a thermostatic expansion valve (TXV) or electronic expansion valve (EEV), the controlled valves can compensate for LL restrictions to some extent. However, for operating conditions in which the valve would otherwise be saturated open or near to open, the restriction will have some impact. Furthermore, some restrictions are so severe that the TXV or EEV is unable to compensate for them most, or all, of the time.

Two definitions of LL fault intensity have been proposed. One definition is a ratio of the pressure drop across the liquid line with a restriction to the unfaulted pressure drop across the liquid line. This definition results in very high intensity values when expressed as a percentage. Another definition is the ratio of the fault-induced change in pressure drop across the liquid line to the total pressure drop from high side to low side (shown in Table 3). This definition has the advantage of having a range from 0 to 100%, and is adopted in the current paper.

It is important to quantify the impacts of LL faults on the performance of an air conditioning system. Several studies (Rossi and Braun, 1997; Breuker and Braun, 1998a, b; Chen and Braun, 2000, 2001; Kim et al., 2006, 2009; Wichman and Braun, 2008, 2009; Payne et al., 2009; Yoon et al., 2011; Domanski et al., 2014; Du et al., 2016; Wang et al., 2016; Kim and Braun, 2020; Hu et al., 2021a, b, c, d, e; Hu and Yuill, 2021, 2022a, b; Hu, 2021) have evaluated the impacts of LL faults in rooftop air conditioners (RTUs), split residential air conditioning systems, and some other types of commercial air conditioners.

Rossi and Braun (1997) and Breuker and Braun (1998a, b) investigated LL fault impacts on a 3-ton RTU with a constant speed reciprocating compressor and an FXO. They imposed four fault intensities (FI) of LL ranging from 5% to 20%. At the LL FI of 20%, cooling capacity and COP decreased by 17.2% and 8.7%, respectively. Chen and Braun (2000, 2001) also studied LL fault impacts on a 5-ton RTU with a constant speed scroll compressor and a TXV. They also implemented four LL FIs ranging from 4.8% to 18.7%. Cooling capacity had almost no change

with LL FI lower than 11% and decreased by about 7% with the maximum LL FI of 18.7%. It demonstrated that the TXV can compensate for some detrimental effects caused by LL faults within the operating range of the TXV. However, when the TXV was fully open (LL FI of 11%), it generated significant impacts on cooling capacity. Wang et al. (2016) imposed LL faults on a 6-ton RTU. With a liquid line pressure drop of around 5.2 bar, cooling capacity and COP reductions up to 27% and 28% were found in this study. Kim and Braun (2020) examined LL faults on a 4-ton RTU with an EEV in the laboratory to test their proposed FDD method but didn't provide the fault impact data.

Some studies (Kim et al., 2006, 2009; Payne et al., 2009; Yoon et al., 2011; Domanski et al., 2014; Du et al., 2016; Hu et al., 2021a, b, c, d, e; Hu and Yuill, 2021, 2022a, b; Hu, 2021) investigated LL fault impacts on residential air conditioning systems. One group (Kim et al., 2006, 2009; Payne et al., 2009; Yoon et al., 2011; Domanski et al., 2014; Du et al., 2016) imposed LL faults on a 2.5-ton split residential heat pump with a scroll compressor and two TXVs (one for cooling and another for heating) in both cooling and heating modes. The FI of LL in cooling mode and heating mode ranged from 0 to 30% and from 5% to 50%, respectively. In cooling mode, COP had almost no change with an LL FI of 10% and decreased by 5% with an FI of 20%. Another group (Hu et al., 2021a, b, c, d, e; Hu and Yuill, 2021, 2022a, b; Hu, 2021) studied LL fault impacts on a 4-ton split residential heat pump with a rotary compressor and a TXV and a 3-ton unitary cooling air conditioner with a scroll compressor and an FXO in cooling mode. Two LL fault intensities (22% and 32% for the heat pump, and 20% and 30% for the air conditioner) were imposed in each system. For the heat pump, cooling capacity and COP had almost no change with LL FI of 22%. However, at the LL FI of 32%, when the TXV was presumably fully open, these two parameters decreased by 7-19% and 6-18% depending on operating conditions. For the air conditioner, cooling capacity and COP decreased by 5-7% and 6-8% for LL FI of 20%, and went down by 16-20% and 17-21% for LL FI of 30%, respectively. Wichman and Braun (2008, 2009) imposed LL faults on a 3-ton walk-in cooler and freezer. With the maximum level of LL faults imposed, capacity decreased up to 55% for the cooler and decreased up to 60% for the freezer. These studies show the importance of detecting LL faults so that they can be addressed.

Rossi and Braun (1997) developed a statistical rule-based (SRB) fault detection and diagnostic (FDD) method to detect five types of faults, including LL, on an RTU equipped with an FXO.

Breuker and Braun (1998a, b) applied this method for RTUs and Kim et al. (2006) applied it for split systems. Chen and Braun (2000, 2001) provided two easy-to-implement FDD methods for a 5-ton RTU with a scroll compressor and a TXV by modifying the SRB method of Rossi and Braun (1997). Li and Braun (2007a, b) developed two methods based on decoupling feature to detect LL faults. One method can be used during the startup of the system. In this method, the refrigerant in the liquid line is assumed be a two-phase mixture for several minutes after startup. Therefore, the temperature difference across the liquid line can be regarded as a decoupling feature to detect LL faults, because any pressure drop will cause a drop in saturation temperature. The second method requires modeling the metering device to obtain the pressure before the metering device, which then can be compared to the measured pressure at the service port of the liquid line. The difference between these two pressures can be used as a decoupling feature. In addition, they also pointed out that, for an air conditioning with a typical subcooling, a significant pressure drop over the liquid line has to occur to generate a phase change of the subcooled refrigerant in the liquid line.

Wichman and Braun (2008, 2009) used the temperature difference over the liquid line to detect LL faults for a 3-ton commercial cooler and freezer. Kim et al. (2009) concluded that single LL faults are sensitive for three parameters: the suction line superheat, temperature difference over the liquid line, and the discharge line temperature. Katipamula et al. (2015) proposed an automated FDD procedure to detect LL faults. Arensmeier et al. (2014) developed remote monitoring and diagnostics tools that include the measurements of the inlet and outlet liquid line temperatures, and ambient temperature to detect LL faults.

Most previous studies investigated LL faults singly, and the FDD methods were developed based on single faults. Faults can occur simultaneously, so the effectiveness of the existing FDD methods when additional faults are present needs further validation. Several studies (Hu et al., 2021b, c, d, e; Hu and Yuill, 2021, 2022b; Hu, 2021, Pelella et al. 2022a, b) have studied simultaneous fault impacts and FDD methods for residential air conditioning systems. Hu et al. (2021b, c, d, e), Hu (2021), and Hu and Yuill (2021, 2022b) experimentally investigated combinations of LL, improper refrigerant charge (CH), improper evaporator airflow (EA), and the presence of non-condensable gas (NC) on two split systems, describing the impacts on performance and features. A virtual refrigerant charge sensor proposed by Li and Braun (2007b) was also tested and validated for application with multiple simultaneous faults, in Hu and Yuill

(2022b). Pelella et al. (2022a, b) investigated simultaneous faults of refrigerant leakages, condenser and evaporator fouling, using both simulation and field study. Fault impacts on system performance and fault detection analysis through pressure and temperature measurements were examined. Based upon the review of existing literature and common field practices, the method of using the temperature drop over the liquid line as the detection feature is of interest because of its practicality and potential for accurate detection. The objective of the current study is to test effectiveness of this decoupling feature to detect LL faults, assign concrete detections thresholds, and understand its applicability and limitations. The premise of this method is that LL fault intensity has to be large enough to generate phase change in the liquid line. In practical applications, faults tend to occur simultaneously, which may affect the effectiveness of this method. Therefore, two similar LL fault intensities (from moderate to severe) were imposed both singly, and in combination with three other common installation faults - CH, EA, and NC - on two different residential systems. One is a 4-ton split heat pump and another is a 3-ton split residential air conditioner. The decoupling feature - liquid line temperature drop - was measured and calculated under various scenarios. Then a sensitivity of this feature to LL faults and the three other faults was analyzed and will be discussed. Finally, the sensitivity of this feature to LL faults in the presence of other faults or fault combinations was also studied. This is the first time the decoupling feature has been tested with combinations of other faults present.

2 Experimental setup and methodology

2.1 Description of tested systems

Table 1 Description of tested systems

System	Nominal capacity (tons)	Compressor	Refrigerant	Expansion device	Accumulator	SEER
I	4	Rotary	R410A	TXV	Yes	18
II	3	Scroll	R410A	FXO	No	13

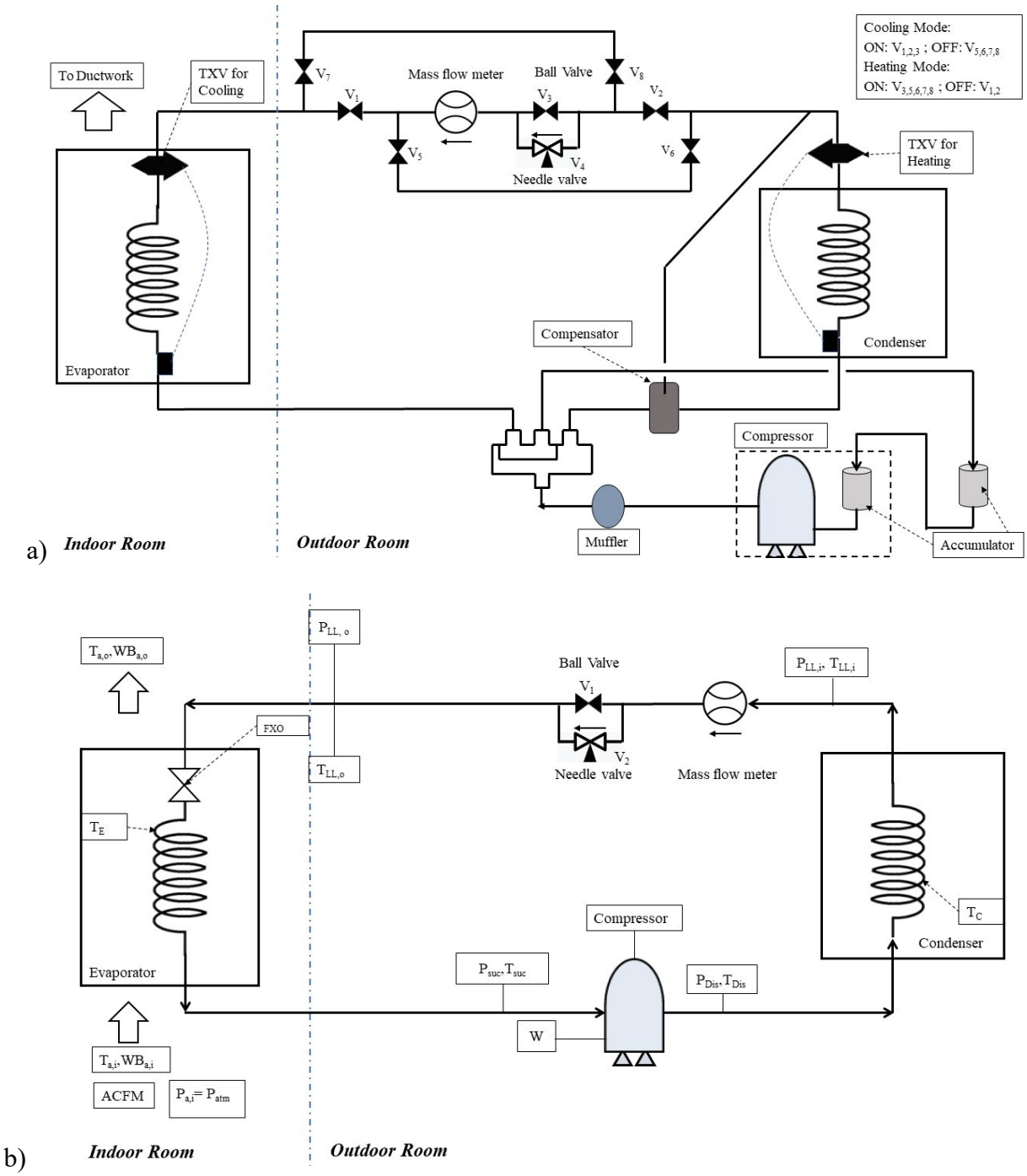

Figure 1. Experimental setup of the tested systems in cooling mode

a) heat pump (Hu et al. 2021a), b) air conditioner (Hu and Yuill 2022a)

A description of the two tested systems is presented in Table 1 and the schematic diagrams of these two systems are presented in Figure 1. System I is an R410A nominal 14 kW (4 ton) split

residential heat pump, rated as 18 seasonal energy efficiency ratio (SEER). It has a rotary compressor, two accumulators, a compensator, a muffler, a reversing valve, and two TXVs (one for heating and another for cooling). It also has an inverter to change the speed of the compressor. We deactivated the controller of the inverter in order to provide uniform operating condition for each test. Both the evaporator and condenser are finned-tube heat exchangers. System II is an R410A nominal 10.6 kW (3 ton) split residential air conditioner, rated as 13 SEER. It contains a single stage constant speed scroll compressor, a microtube condenser, and an FXO. Both the evaporator and condenser are also finned tube heat exchangers.

2.2 Test conditions

The operation testing conditions for the heat pump and air conditioner in cooling mode are presented in Table 2 (the D condition was not tested for the air conditioner).Two of these conditions are from the rating conditions specified in AHRI Standard 210/240 (2017). The test matrix covers four categories: the first three conditions are wet-coil tests, in which only the outdoor dry-bulb temperature varies, while the last condition is a dry evaporator coil test. The test matrix of intensities for each fault for both the heat pump and air conditioner is presented in

Table 3. The fault intensity for the air-conditioner was slightly different from the heat pump for some cases of LL and NC, due to the practical difficulties of imposing these faults, and the most intense EA fault could not be applied due to system operating limits for the air-conditioner. Where air-conditioner values were different from the heat pump, the intensities are indicated within square brackets.

Table 2 Operating conditions in cooling mode

Test condition	Indoor room temperature (°C)		Outdoor room temperature (°C)
	Dry-bulb	Wet-bulb	Dry-bulb
A*	26.7	19.4	35.0
B*		19.4	27.8
C		19.4	40.5
D		<13.3	35.0

* correspond to rating conditions used in AHRI Standard 210/240 (2017).

Table 3 Test matrix for selected faults

Fault	Abbreviation	Definition of intensity	Fault intensity (%)
Improper evaporator airflow	EA	$\frac{\dot{V}_{EA,actul}}{\dot{V}_{EA,rated}}$	60 [**], 80, 100,120
Improper refrigerant charge	CH	$\frac{m_{ref,actual}}{m_{ref,rated}}$	70, 80, 100,120
Liquid line restriction	LL	$\frac{\Delta P_{LL,actual,A} - \Delta P_{LL,rated,A}}{\Delta P_{comp,rated,A}}$	0, 22 [20], 32 [30]
Non-condensable gas	NC	$\frac{P_{N_2,35°C}}{\Delta P_{atm}}$	0, 49, 105 [99]

"**" Not tested for air conditioner

"[]" Values in the square brackets indicate a different fault intensity for the air conditioner

To decrease the test dimensions for simultaneous faults, only single fault scenarios were tested in all operating conditions. To reduce the test matrix for simultaneous faults, we tested multiple simultaneous fault combinations only at the rating "A" operating condition: 35 °C outdoors with 26.7 °C indoor dry bulb and 19.4 °C indoor wet bulb.

Table 4 Fault notation, intensity, and simultaneous combinations

Fault categories		
Fault	Intensities (%)	Notation
EA	60 [**], 80, 100, 120	EA60 [**], EA80, EA100, EA120
CH	70, 80,100,120	CH70, CH80, CH100, CH120
LL	0, 22 [20], 32 [30]	LL0, LL22 [LL20], LL32 [LL30]
NC	0, 49, 105 [99]	NC0, NC49, NC105 [NC99]
Double-fault combinations		
Combination	Number of tests	Example
EA, CH	9 [6]	EA80 + CH120
EA, LL	6 [4]	EA80 + LL22 [LL20]
EA, NC	6 [4]	EA120 + NC49
CH, LL	6 [5]	CH120 + LL32 [LL32]
CH, NC	6	CH80 + NC49
LL, NC	4	LL22 [LL20] + NC49
Triple-fault combinations		
Combination	Number of tests	Example
EA, CH, LL	18 [10]	EA80 + CH120 + LL32 [LL30]
EA, CH, NC	18 [12]	EA80 + CH80 + NC49
EA, LL, NC	12 [8]	EA120 + LL22 [LL20] + NC49
CH, LL, NC	8 [6]	CH80 + LL22 [LL20] + NC49
Quadruple-fault combinations		
Combination	Number of tests	Example
EA, CH, LL, NC	24 [12]	EA80 + CH80 + LL22 [LL20] + NC49

"**" Not tested for air conditioner

"[]" Values in the square brackets indicate different fault intensity and numbers of tests for the air conditioner

Table 4 describes the fault intensities for each of the four fault types, and includes the fault-free condition (100% for EA and CH; 0% for LL and NC). For the heat pump, there are 133 possible combinations of fault condition from this set: 37 double; 60 triple; and 36 quadruple; while for the air conditioner, there are 98 possible combinations of fault condition from this set: 30 double; 44 triple; and 24 quadruple. Some of these combinations could not be tested, because they exceed the safe operating bounds for the system. For example, the combination CH70, NC49, and LL32 (LL30 for the air conditioner) caused the discharge temperature to exceed the manufacturer's limit of 105 °C. The remaining numbers of test conditions for the heat pump and air conditioner are 117 and 77, respectively. Each test was conducted over a period of at least 10 minutes after steady state conditions had been reached, and the measurements (taken on one second intervals) were averaged to provide the results in this study. Table 4 gives a count of each fault combination of fault types within the 117 results for the heat pump, and the 77 results for the air conditioner. The figures in the results (Section 3) use a combination of the abbreviation and fault intensity to represent the fault. For instance, EA80 represents the evaporator airflow rate at 80% of the nominal level.

2.3 Calculation method

The premise for detecting liquid line restriction faults is that some of the refrigerant in the liquid line must experience phase change as a consequence of the pressure drop through the restriction. Otherwise, the temperature change across the liquid line should typically be minor. There is little heat transfer in the liquid line, because: (a) it is normally insulated, as was the case in the experimental setup; and (b) the refrigerant in this part of the cycle is close to the ambient temperature. In contrast, when phase change begins to occur, the temperature difference across the liquid line is significant. The following equation defines the temperature difference, ΔT_{LL}, over the liquid line.

$$\Delta T_{LL} = T_{LL,i} - T_{LL,o} \tag{1}$$

where $T_{LL,i}$ and $T_{LL,o}$ are the inlet and outlet temperatures of the liquid line, respectively, °C.

Figure 2 depicts the sensors that are installed in the liquid line at the rating "A" operating condition (AHRI 210/240, 2017). By adjusting the position of valves 1 and 2, the LL fault can be imposed and controlled to the fault intensities shown in Table 5.

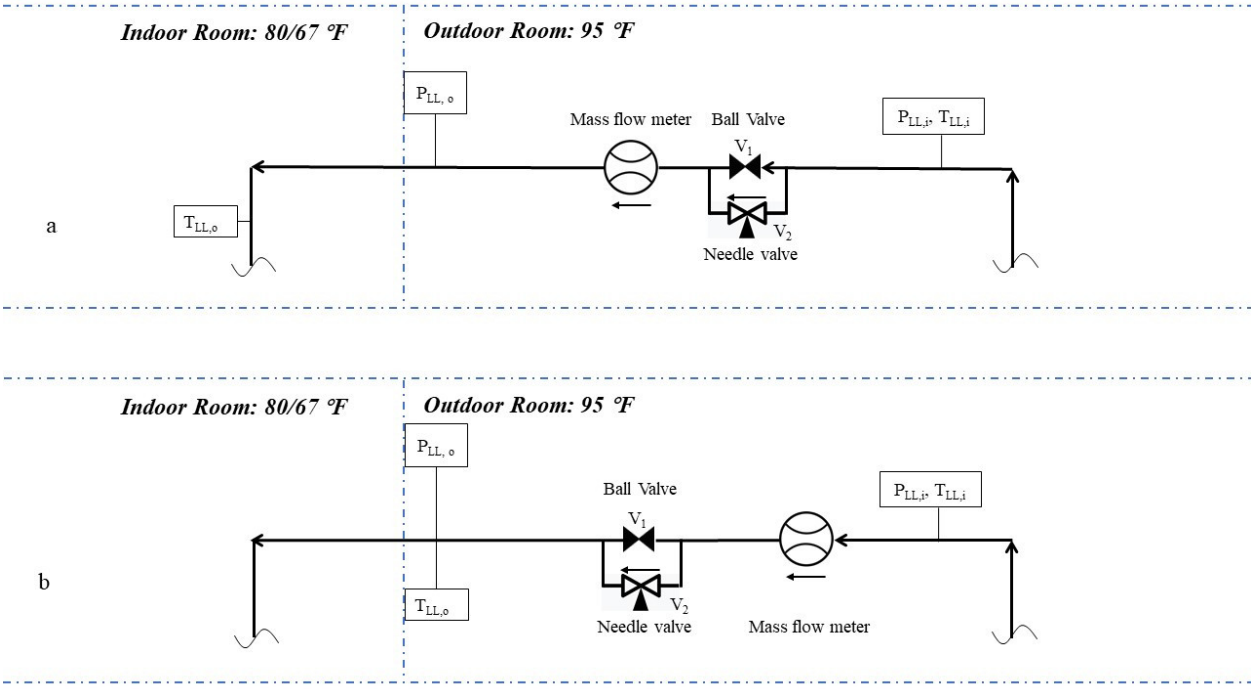

Figure 2. Temperature and pressure sensors on the liquid line

a) heat pump, b) air conditioner

Table 5 State changes for varying LL fault intensity at rating "A" testing condition

System	Fault	ΔP	$\dot{m}_{ref}$	T_{SC}	$T_{LL,i}$	$T_{LL,o}$	ΔT_{LL}	Valve position [% open]	
		kPa	kg/min	°C	°C	°C	°C	V_1	V_2
I	LL0	62	4.56	6.7	37.3	36.8	0.5	100%	0
	LL22	441	4.34	6.8	37.2	35.2	1.9	0	100%
	LL32	607	3.60	6.8	36.4	31.1	5.3	0	50%
II	LL0	21	3.62	4.1	38.8	38.6	0.2	100%	0
	LL20	362	3.10	6.8	36.7	36.4	0.4	0	50%
	LL30	538	2.56	8.2	35.8	33.7	2.0	0	25%

Table 5 presents the detailed temperature drops and other state changes for each LL fault intensity at the A test condition for both systems. When there is no LL fault (LL0), the refrigerant enters and exits the liquid line as a subcooled liquid. The stray heat loss to the environment in the fault-free case caused the temperature to decrease along the liquid line by 0.5 °C for the heat pump and 0.2 °C for the air-conditioner. At the first and second levels of LL fault, the refrigerant mass flow rates are less than or equal to the fault-free condition, so a slight increase in ΔT_{LL} may be

attributable to increased transit time for the refrigerant. However, for System I, the ΔT_{LL} for LL22 and LL32 are 1.9 °C, 5.3 °C, respectively, indicating that phase change must have occurred along the liquid line. In contrast, for System II, the ΔT_{LL} for LL20 and LL30 are 0.4 °C, 2.0 °C, respectively, indicating that phase change must have occurred along the liquid line for the air conditioner at the higher fault level only (LL30).

The LL fault feature, ΔT_{LL}, is not used as a detection feature for other fault types, to the authors' knowledge. Common diagnostic features or methods for the other faults are as follows. Since airflow often can be easily measured, EA faults can be detected by comparing the actual airflow rate to a target airflow rate. The actual airflow rate can be measured using a flow plate (Francisco and Palmiter, 2003), or virtual methods (Hjortland and Braun, 2016). CH faults are commonly diagnosed by comparing suction superheat or subcooling quantities to a target value, or with more advanced methods such as a virtual charge sensor (Li and Braun, 2007b), which use both superheat and subcooling, as well as some system characterization parameters. NC faults can be diagnosed by comparing the difference between saturation temperature at the measured system pressure with the measured temperature (Hu and Yuill, 2022c).

3 Results and discussion

3.1 Single faults

To show all the single fault ΔT_{LL} results in one plot, Table 6 defines short labels for levels of each fault at each fault intensity. L-0 represents the no fault for each fault type. L-3 is undefined for LL and NC faults. The levels are ordered so as to improve the readability of Figure 3.

Table 6 The relationship between fault intensity and levels

Levels	Fault intensity			
	EA (%)	CH (%)	LL (%)	NC (%)
L-3	120	120	-	-
L-0	100	100	0	0
L-1	80	80	22 [20]	49
L-2	60 (**)	70	32 [30]	105 [99]

"**" Not tested for air conditioner

"[ ]" Values in the square brackets indicate different fault intensity for air conditioner

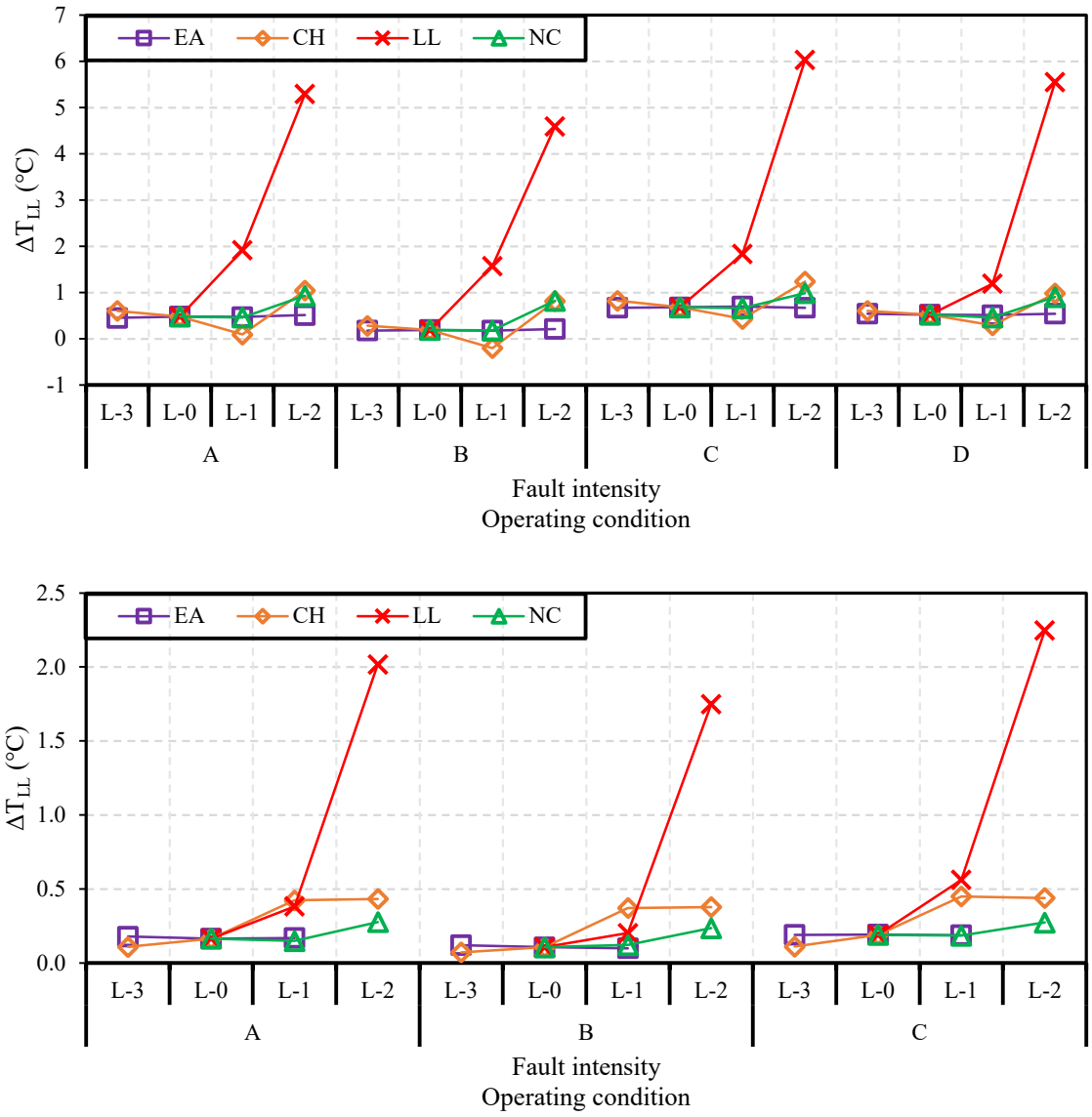

Figure 3. Temperature difference across liquid line under single fault conditions

a) heat pump, b) air conditioner

Figure Figure 3 presents ΔT_{LL} for single faults (EA, CH, LL, and NC) at each of the levels defined in Table 6, and each of the four operating conditions (A to D, D was not tested for the air conditioner) It shows that ΔT_{LL} is only sensitive to LL faults, and insensitive to other faults (within ±1.5 °C for heat pump and within ±0.5 °C for air conditioner). Since the first level of single LL fault has almost no impact on cooling capacity and COP for the heat pump, the threshold for detecting LL faults can be set as ΔT_{LL} > 1.5 °C for single faults. The dry-evaporator test (D, on the right side of the plot) is relatively insensitive at the first level of LL faults compared to wet-coil

tests (A, B, and C). The first level of LL fault for the air conditioner decreased cooling capacity by 6% and COP by 7%. Therefore, the threshold for detecting LL faults can be set as $\Delta T_{LL} > 0.5$ °C for single scenarios.

3.2 Simultaneous faults

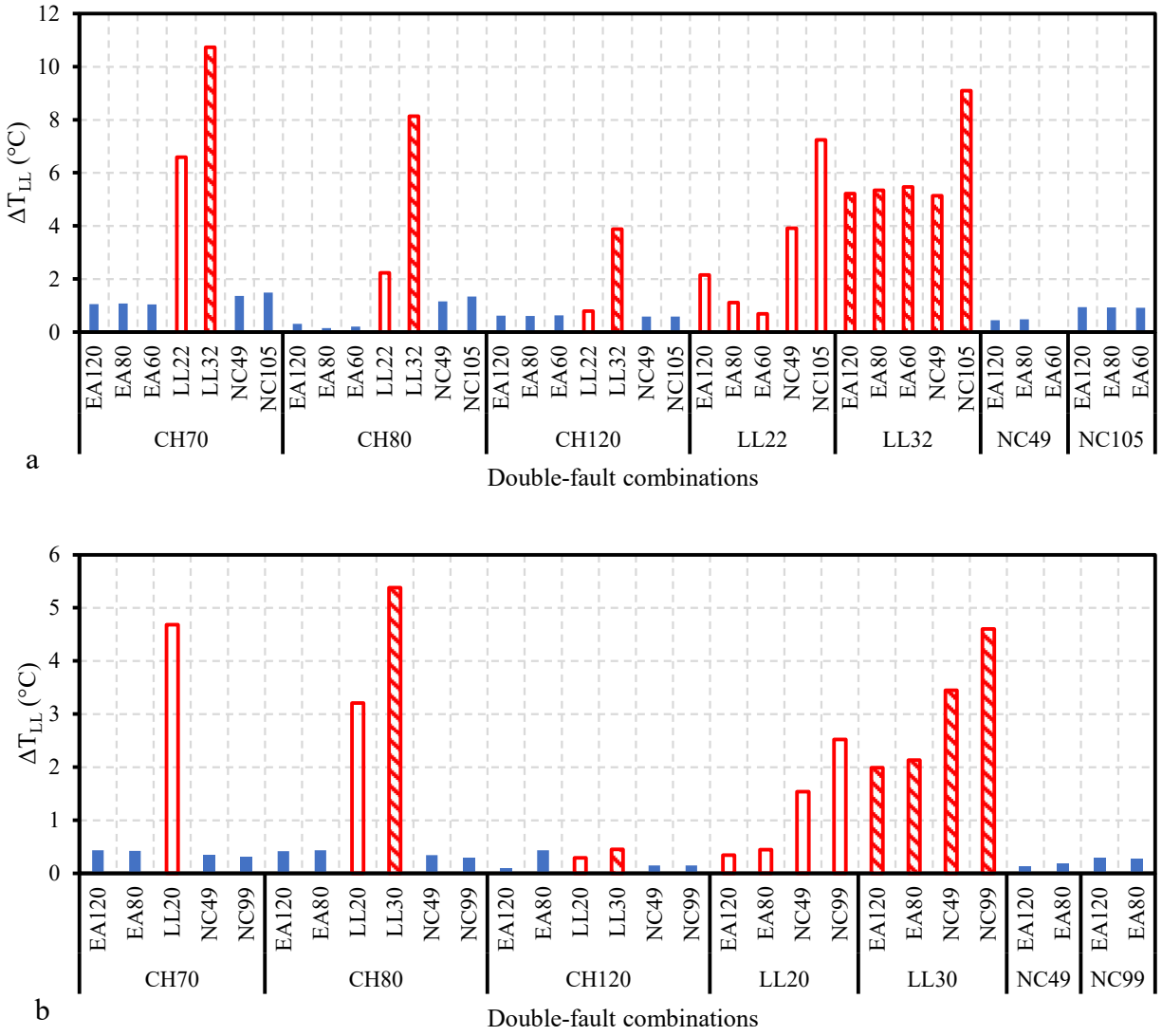

Figure 4. Temperature difference across liquid line with two faults

a) heat pump, b) air conditioner

Figure 4 presents ΔT_{LL} for the double-fault combinations. The presentation of the figure is different from Figure 3 because an additional dimension of data is represented – fault type combinations.

All combinations that include an LL fault are presented in red (unhatched is the first level of LL faults and hatched is the second level of LL faults). Also, for the combined faults, all tests were conducted at the A operating condition, so these results are presented more compactly than Figure 3.

The critical question is whether other faults can confound the diagnostic feature, ΔT_{LL}, to either mask an LL fault, or to make it appear that there is an LL fault when there isn't one. In most cases, ΔT_{LL} is insensitive to combinations of non-LL faults (less than 1.5 °C for the heat pump, and less than 0.5 °C for the air conditioner). For heat pump, the sensitivity of ΔT_{LL} to LL faults is reduced in the presence of low evaporator airflow (EA60 and EA80) and OC faults, especially for the first level of LL fault. However, for the second level of LL fault (LL32), ΔT_{LL} is still significantly impacted, even in the presence of those two faults. For air conditioner, the sensitivity of ΔT_{LL} to LL faults is reduced in the presence of OC faults, even for the second level of LL faults (LL30). UC or NC faults increase the sensitivity of ΔT_{LL} to LL faults for both heat pump and air conditioner. For instance, for the first levels of LL and NC faults individually, ΔT_{LL} for heat pump is 1.9 °C and 0.5 °C, respectively. However, when combined, ΔT_{LL} of these two combinations is 3.9 °C, increasing by 1.5°C. Therefore, if the presence of other faults is known, the threshold can be adjusted.

Figure 5 shows the temperature difference across the liquid line under various triple fault combinations for both heat pump and air conditioner. ΔT_{LL} is still insensitive to combinations of the other three faults (EA, CH, and NC); its value is always less than 1.5 °C for the heat pump and less than 0.5°C for the air conditioner. For the heat pump, regarding combinations with LL22, all other fault combinations show ΔT_{LL} remains sensitive, except for CH120 (OC). Since overcharge tends to increase subcooling, it is not surprising that there would be less likelihood of an LL fault causing phase change, hence increasing ΔT_{LL}. However, ΔT_{LL} is sensitive to all combinations with LL32, even OC faults. For air conditioner, OC will still reduce the sensitivity of ΔT_{LL} to LL faults, except for the combinations of LL30 combined with NC faults.

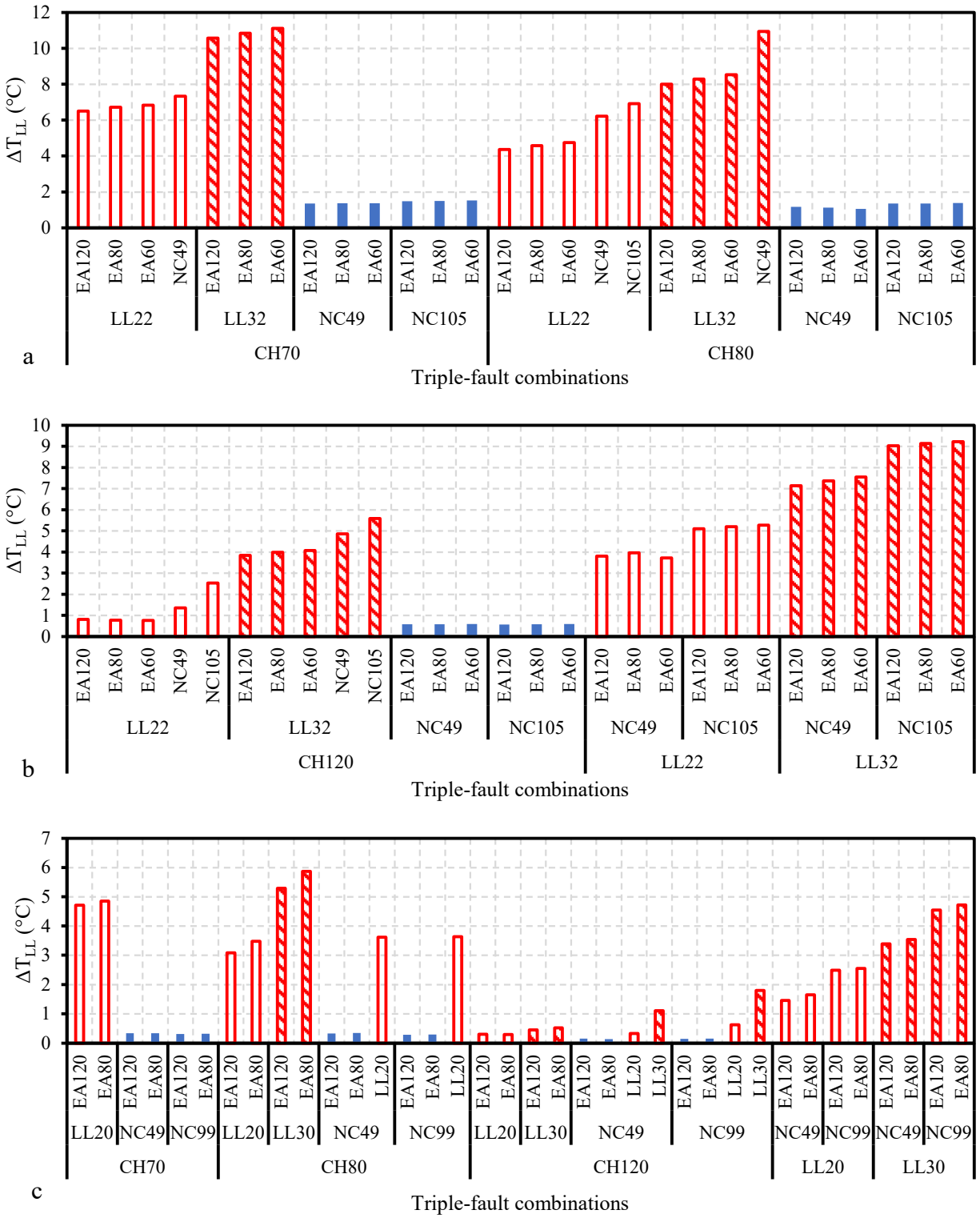

Figure 5. Temperature difference across liquid line with three faults

a, b) heat pump, c) air conditioner

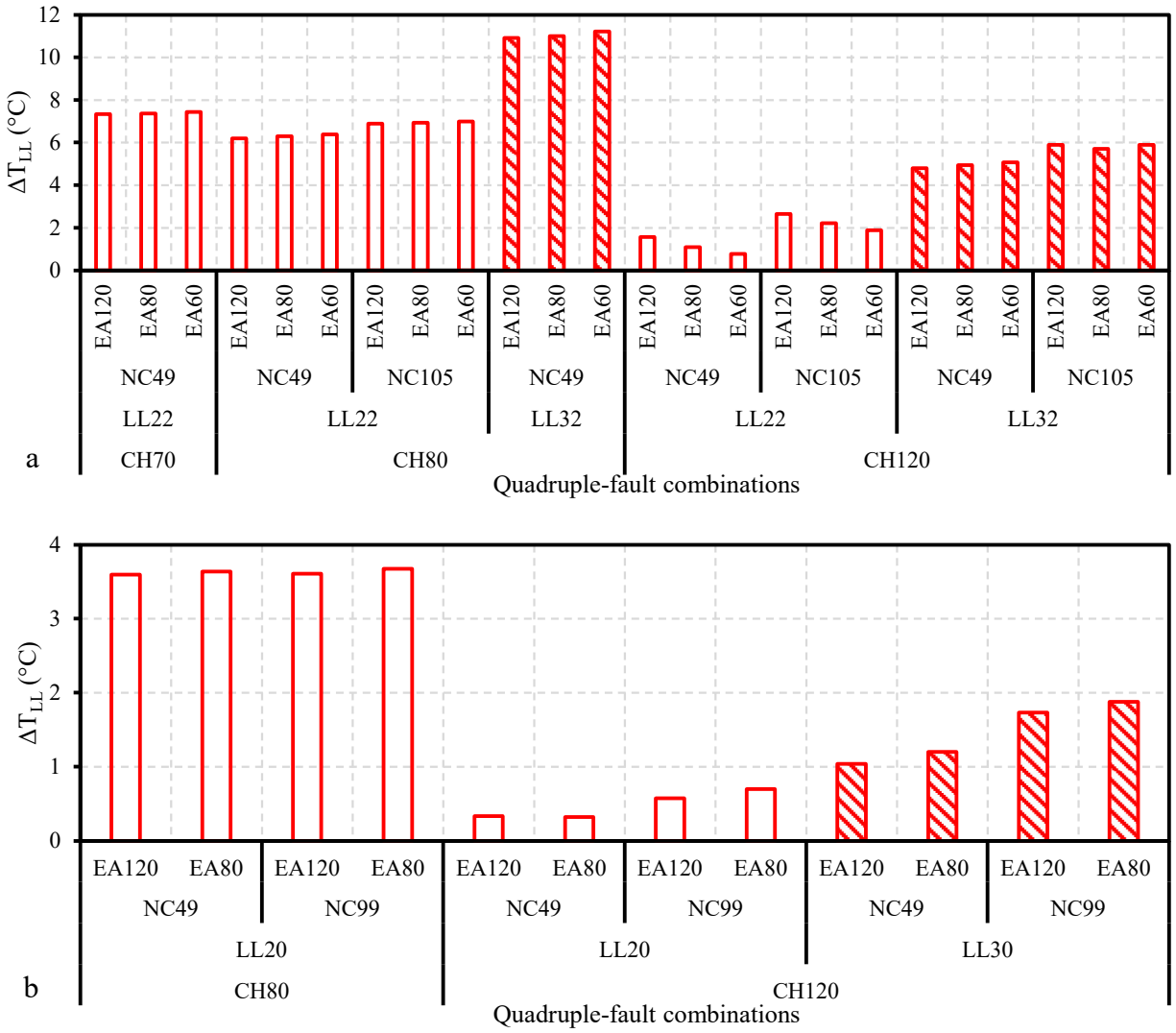

Figure 6. Temperature difference across liquid line with four faults

a) heat pump, b) air conditioner

Figure 6 presents ΔT_{LL} for quadruple-fault combinations for both the heat pump and air conditioner. Fault combinations with CH120 still reduce the sensitivity of ΔT_{LL} to LL faults, especially, for the first level of LL fault. For the more severe faults (LL32 for the heat pump and LL30 for the air conditioner), even with overcharge, the ΔT_{LL} is very sensitive to LL faults.

4 Conclusions

The temperature difference across the insulated liquid line of a split heat pump system and air conditioner was investigated for single faults under different operating conditions, and for simultaneous double, triple, and quadruple fault combinations under the "A" operating condition. This temperature difference is considered for a decoupling feature to use in diagnosing liquid line restrictions. From an analysis of the measurement data, the following conclusions can be drawn:

- A threshold of 0.5 °C for the FXO-equipped system and 1.5 °C for the TXV-equipped system successfully differentiates scenarios with an LL fault. These thresholds are close to the first LL fault level in this study. For the air-conditioner this was LL20, which is associated with a reduction of COP of 5-7% (Hu and Yuill, 2022a). For the heat pump, this first fault level, LL22, caused a negligible reduction in COP (Hu et al., 2021a).
- Importantly, the decoupling feature - temperature difference across the liquid line - is insensitive to non-LL faults (individually or combined). In application of fault diagnostics, this means that other faults would not be misdiagnosed as an LL fault, and that the LL fault can still be diagnosed, even when other faults are present.
- This feature was more significantly impacted when LL faults were combined with UC or NC faults, and less pronounced in the presence of OC faults. It was not impacted when in combination with EA faults.
- This feature is not very effective with light LL faults, because such faults may not bring about phase change in the liquid line. However, these light faults also will not be very impactful on performance.
- The feature can be used effectively and reliably for detection of moderate and severe LL faults for both TXV-equipped and FXO-equipped systems.

Acknowledgements:

This work was supported by the Building America program of the U.S. Department of Energy's Office of Energy Efficiency and Renewable Energy (EERE) under the Building Technologies Office agreement DE-EE0008689. We are grateful to Dave Coziahr for his expertise and assistance with system installations.

References

[1]. EIA (2015). 2015 Residential energy consumption survey. U.S. Energy Information Administration (EIA). https://www.eia.gov/consumption/residential/data/2015

[2]. Rossi, T. M. & Braun, J. E., 1997, A statistical, rule-based fault detection and diagnostic method for vapor compression air conditioners, HVAC&R Res., 3 (1) (1997) 19–37. https://doi.org/10.1080/10789669.1997.10391359

[3]. Breuker, M.S., & Braun, J.E., 1998a, Common faults and their impacts for rooftop air conditioners, HVAC&R Res., 4 (3) (1998) 303-318. https://doi.org/10.1080/10789669.1998.10391406.

[4]. Breuker, M.S. & Braun, J.E., 1998b, Evaluating the performance of a fault detection and diagnostic system for vapor compression equipment, HVAC&R Res., 4(4) (1998) 401-425. https://doi.org/10.1080/10789669.1998.10391412.

[5]. Chen, B. & Braun, J.E., 2000, Simple fault detection and diagnostics methods for packaged air conditioners. Proc. 8th Int. Refrig. Conf., Paper 498, West Lafayette, IN, USA, July 25-28, 2000. https://docs.lib.purdue.edu/iracc/498.

[6]. Chen, B. & Braun, J.E., 2001, Simple rule-based methods for fault detection and diagnostics applied to packaged air conditioners. ASHRAE Trans., 107 (2001) 847-857.

[7]. Kim, M, Payne, W.V., Domanski, P.A., Hermes, C.J.L, 2006, Performance of a Residential Heat Pump Operating in the Cooling Mode with Single Faults Imposed, NISTIR 7350, NIST, Gaithersburg, MD, USA, 2006. https://dx.doi.org/10.6028/NIST.IR.7350.

[8]. Kim, M., Payne,W.V., Domanski, P.A., Yoon, S.H., Hermes, C.J.L., 2009, Performance of a residential heat pump operating in the cooling mode with single faults imposed. Appl. Therm. Eng., 29 (4) (2009) 770–778. https://doi.org/10.1016/j.applthermaleng.2008.04.009.

[9]. Wichman, A. and Braun, J. E. (2008). Fault Detection and Diagnostics for Commercial Coolers and Freezers. Int. Refrig. Air Cond. Conf. Paper 919. https://docs.lib.purdue.edu/iracc/919

[10]. Wichman A., Braun J.E., 2009., Fault Detection and Diagnostics for Commercial Coolers and Freezers. HVAC&R Res., 15 (1) (2009) 77-99. https://doi.org/10.1080/10789669.2009.10390826

[11]. Payne, W.V., Yoon, S.H., Domanski, P.A., 2009, Heating mode performance measurements for a residential heat pump with single-faults imposed, Technical Note 1648, NIST, Gaithersburg, MD, USA, 2009. https://doi.org/10.6028/NISTPUB.0413171251.

[12]. Yoon, S.H., Payne, W.V., Domanski, P.A., 2011, Residential heat pump heating performance with single faults imposed, Appl. Therm. Eng., 31 (5) (2011) 765–771. https://doi.org/10.1016/j.applthermaleng.2010.10.023

[13]. Cho, J.M., Heo, J., Payne,W.V., Domanski, P.A., 2014, Normalized performance parameters for a residential heat pump in the cooling mode with single faults imposed. Appl. Therm. Eng., 67 (1) (2014) 1–15. https://doi.org/10.1016/j.applthermaleng.2014.03.010.

[14]. Domanski, P.A., Henderson, H.I., Payne,W.V. 2014, Sensitivity analysis of installation faults on heat pump performance. NIST Technical Note 1848, NIST, Gaithersburg, MD, USA, 2014. http://dx.doi.org/10.6028/NIST.TN.1848.

[15]. Du, Z., Domanski, P.A., Payne, W.V., 2016, Effect of common faults on the performance of different types of vapor compression systems, Appl. Therm. Eng., 98 (2016) 61–72. https://doi.org/10.1016/j.applthermaleng.2015.11.108.

[16]. Wang, J., Gorbounov, M., Yasar, M., Reeve, H., Hjortland, A. L., Braun, J. E., 2016, Lab and Field Evaluation of Fault Detection and Diagnostics for Advanced Roof Top Unit. Int. Refrig. Air Cond. Conf. Paper 1590. http://docs.lib.purdue.edu/iracc/1590.

[17]. Kim, W., Braun, J.E., 2020, Development, implementation, and evaluation of a fault detection and diagnostics system based on integrated virtual sensors and fault impact models. Energy Build., 226 (2020), 110368. https://doi.org/10.1016/j.enbuild.2020.110368.

[18]. Hu, Y., Yuill, D. P., Ebrahimifakhar, A., Rooholghodos, A., 2021a, An experimental study of the behavior of a high efficiency residential heat pump in cooling mode with common installation faults imposed. Appl. Therm. Eng., 184 (2021), 116116. https://doi.org/10.1016/j.applthermaleng.2020.116116.

[19]. Hu, Y., Yuill, D. P., Ebrahimifakhar, A., Rooholghodos, S.A., Chen, Y., 2021b, Impacts of simultaneous operating faults on cooling performance of a high efficiency residential heat pump. Energy Build., 242 (2021),110975. https://doi.org/10.1016/j.enbuild.2021.110975.

[20]. Hu, Y.; Yuill, D. P.; Chen, Y., 2021c. Impacts and Detection of Non-Condensable Gas in a Residential Air Source Heat Pump. 18th Int. Refrig. Air Cond. Conf. at Purdue, Paper 2244, West Lafayette, IN, USA, May 24-28. https://docs.lib.purdue.edu/iracc/2244.

[21]. Hu, Y.; Yuill, D. P.; Chen, Y., 2021d. Experimental Quantification of Liquid Line Temperature Drop as a Feature to Detect Liquid Line Restriction Faults in a Residential Heat Pump. 18th Int. Refrig. Air Cond. Conf. at Purdue, Paper 2245, West Lafayette, IN, USA, May 24-28. https://docs.lib.purdue.edu/iracc/2245

[22]. Hu, Y., Yuill, D.P., Rooholghodos, S.A., 2021e. Interactions between Refrigerant Charge Level and Other Installation Faults on the Behavior of a Residential Heat Pump in Cooling Mode. 18th Int. Refrig. Air Cond. Conf. at Purdue, Paper 2246, West Lafayette, IN, USA, May 24-28. https://docs.lib.purdue.edu/iracc/2246

[23]. Hu, Y., Yuill, D. P., 2021, Effects of multiple simultaneous faults on characteristic fault detection features of a heat pump in cooling mode. Energy Build., 251 (2021), 111355. https://doi.org/10.1016/j.enbuild.2021.111355.

[24]. Hu, Y., 2021, Development and demonstration of a method to determine residential air-conditioning system fault prevalence. Ph.D. thesis, Durham School of Architectural Engineering and Construction, University of Nebraska-Lincoln, Omaha, NE, USA, 2021.

[25]. Hu, Y., Yuill, D.P., 2022a, Impacts of common faults on an air conditioner with a microtube condenser and analysis of fault characteristic features. Energy Build., 254 (2022), 111630. https://doi.org/10.1016/j.enbuild.2021.111630.

[26]. Hu, Y., Yuill, D.P., 2022b, Multiple simultaneous faults' impacts on air-conditioner behavior and performance of a charge diagnostic method. Appl. Therm. Eng., 215 (2022), 119015. https://doi.org/10.1016/j.applthermaleng.2022.119015.

[27]. Li, H. & Braun, J. E., 2007a. Decoupling Features and Virtual Sensors for Diagnosis of Faults in Vapor Compression Air Conditioners. Int. J. Refrig., 30 (3), 546-564. https://doi.org/10.1016/j.ijrefrig.2006.07.024.

[28]. Li, H. & Braun, J. E., 2007b. A Methodology for Diagnosing Multiple-Simultaneous Faults in Vapor Compression Air Conditioners. HVAC&R Res., 13 (2), 369-395. https://doi.org/10.1080/10789669.2007.10390959

[29]. Katipamula, S., Kim, W., Lutes, R.G., Underhill, R.M. Rooftop unit embedded diagnostics: automated fault detection and diagnostics (AFDD) development, field testing and validation. Tech. rep., Pacific Northwest National Laboratory, Report PNNL-23790, Richland, WA, 2015. https://www.pnnl.gov/main/publications/external/technical_reports/PNNL-23790.pdf

[30]. Arensmeier, J. N., Hemmelgarn, G.M., Alsaleem, F. M., Abiprojo, P. (2014). HVAC system remote monitoring and diagnosis. US Patent No. 9638436B2.

[31]. Pelella, F., Viscito, L., Mauro, A.W. (2022a). Combined effects of refrigerant leakages and fouling on air-source heat pump performances in cooling mode. App. Therm. Eng., 204 (2022), 117965. https://doi.org/10.1016/j.applthermaleng.2021.117965.

[32]. Pelella, F., Viscito, L., Mauro, A.W. (2022b). Soft faults in residential heat pumps: Possibility of evaluation via on-field measurements and related degradation of performance. Energy Convers. and Manag., 260 (2022), 115646. https://doi.org/10.1016/j.enconman.2022.115646.

[33]. AHRI, 2017, Performance Rating of Unitary Air-conditioning & Air-source Heat Pump Equipment. AHRI Standard 210/240-2017, Air-Conditioning & Refrigerant Institute, Arlington, VA, USA, 2017. http://www.ahrinet.org/App_Content/ahri/files/STANDARDS/AHRI/AHRI_Standard_210-240_2017.pdf.

[34]. Francisco, P.W. & Palmiter, L., 2003, Field Evaluation of a New Device to Measure Air Handler Flow, ASHRAE Trans., (2003) 403-412.

[35]. Hu, Y., Yuill, D. P.(2022c). Non-condensable gas in the refrigerant of air-source heat pumps: interactions between detection features, charge level, and temperature. Int. J. Refrig., https://doi.org/10.1016/j.ijrefrig.2022.10.006.

[36]. Hjortland, A.L, Braun, J.E. (2016) Virtual sensors for rooftop unit air-side diagnostics, Sci. Technol. Built Env., 22:2, 189-200, DOI: 10.1080/23744731.2016.1124715